

Comparison of helper component-protease RNA silencing suppression activity, subcellular localization, and aggregation of three Korean isolates of *Turnip mosaic virus*

Jae-Yeong Han¹ · Jinsoo Chung¹ · Jungkyu Kim¹ · Eun-Young Seo¹ · James P. Kilcrease² · Gary R. Bauchan³ · Seungmo Lim^{4,5} · John Hammond² · Hyoun-Sub Lim¹

Received: 25 November 2015 / Accepted: 29 March 2016 / Published online: 8 April 2016
© Springer Science+Business Media New York (outside the USA) 2016

Abstract In 2014, we performed a nationwide survey in Korean radish fields to investigate the distribution and variability of *Turnip mosaic virus* (TuMV). *Brassica rapa* ssp. *pekinensis* sap-inoculated with three isolates of TuMV from infected radish tissue showed different symptom severities, whereas symptoms in *Raphanus sativus* were similar for each isolate. The helper component-protease (HC-Pro) genes of each isolate were sequenced, and phylogenetic analysis showed that the three Korean isolates were clustered into the basal-BR group. The HC-Pro proteins of these isolates were tested for their RNA silencing suppressor (VSR) activity and subcellular localization in *Nicotiana benthamiana*. A VSR assay by co-agroinfiltration

of HC-Pro with soluble-modified GFP (smGFP) showed that HC-Pro of isolate R007 and R041 showed stronger VSR activity than R065. The HC-Pro showed 98.25 % amino acid identity, and weak VSR isolate (R065) has a single variant residue in the C-terminal domain associated with protease activity and self-interaction compared to isolates with strong VSR activity. Formation of large subcellular aggregates of GFP:HC-Pro fusion proteins in *N. benthamiana* was only observed for HC-Pro from isolates with strong VSR activity, suggesting that R065 ‘weak’ HC-Pro may have diminished self-association; substitution of the variant C-terminal residue largely reversed the HC-Pro aggregation and silencing suppressor characteristics. The lack of correlation between VSR efficiency and induction of systemic necrosis (SN) suggests that differences in viral accumulation due to HC-Pro are not responsible for SN.

Edited by Karel Petrzik.

Electronic supplementary material The online version of this article (doi:10.1007/s11262-016-1330-1) contains supplementary material, which is available to authorized users.

✉ John Hammond
john.hammond@ars.usda.gov; john.hammond@usda.ars.gov

✉ Hyoun-Sub Lim
hyounlim@cnu.ac.kr

¹ Chungnam National University, Daejeon, Republic of Korea

² Floral and Nursery Plants Research Unit, USDA-ARS, USNA, Beltsville, MD 20705, USA

³ Electron and Confocal Microscopy Unit, USDA-ARS, BARC, Beltsville, MD 20705, USA

⁴ Plant Systems Engineering Research Center, Korea Research Institute of Bioscience & Biotechnology, Daejeon 305-806, Republic of Korea

⁵ Biosystems and Bioengineering Program, University of Science and Technology, Daejeon 305-350, Republic of Korea

Keywords *Turnip mosaic virus* · Helper component-protease (HC-Pro) · RNA silencing suppressor efficiency · Pathogenicity

Turnip mosaic virus (TuMV; genus *Potyvirus*, family *Potyviridae*) has a c.10 kb plus-sense RNA genome and infects over 318 plant species in 156 genera from 43 families, especially in *Brassicaceae*; only *Cucumber mosaic virus* is more important in vegetables worldwide [1–6]. TuMV is transmitted non-persistently by many aphid species [6]. Potyvirus helper component-protease (HC-Pro) functions include aphid-mediated virus transmission; RNA amplification; systemic movement; suppression of post-transcriptional RNA silencing; and C-terminal self-cleaving proteinase [7, 8]. Three major HC-Pro domains correspond approximately to the N-terminal 100, central 200, and C-terminal 150 residues [9]. An N-terminal KITC motif binds aphid stylets [10] and a

C-terminal PTK triplet binds to DAG in the coat protein N-terminus [11, 12]. The central domain affecting RNA silencing suppression, genome amplification, synergism with other viruses, and systemic movement includes conserved FRNK, IGN (LAIGN), and CCC motifs [13–15] and other residues associated with non-specific RNA binding [16].

Due to its many hosts worldwide, there is interest in the evolution of TuMV isolates with differential host ranges. Two major groups are known; B-type isolates mainly infect *Brassica* species, but not radish (*Raphanus sativus*), while BR-type isolates infect both *Brassica* and *Raphanus* [17, 18]. The Asian-BR group includes many Asian isolates, but basal-BR isolates are emerging in Asia [19, 20]. Strains are defined in part by host resistance genes, and by viral pathogenicity determinants [2, 3, 18, 19, 21, 22] which remain poorly defined; HC-Pro variation has been implicated in differences between horseradish strains [23].

We have shown that replication and symptom severity of a potyvirus, *Alternanthera mosaic virus*, are significantly affected by a single residue change in the Triple Gene Block 1 protein viral suppressor of RNA silencing (VSR) [24]. Here we examine VSR function and subcellular localization of HC-Pro of TuMV isolates from radish, an important crop in Korea, in relation to symptom expression to determine whether the TuMV VSR has similar effects on disease severity.

TuMV isolates R007, R041, and R065 were selected from *R. sativus* in Korea [25] based on differential symptoms in *R. sativus*, *B. rapa* ssp. *pekinensis* (Chinese cabbage), and *Nicotiana benthamiana*. Each isolate induced mild mosaic and mottle in *R. sativus* at 11–20 days post inoculation (dpi) (Suppl. Fig. 1). However, in Chinese cabbage isolates R041 and R065 induced systemic necrosis (SN) by 20 dpi, with plants dead or nearly dead at 30 dpi, while plants inoculated with R007 developed systemic mottle or mosaic without SN by 20 dpi, remaining so at 30 dpi (Fig. 1a). R041 and R065 induced SN in *N. benthamiana* while R007 caused only mild mosaic [25].

HC-Pro genes of each isolate were cloned and sequenced (Macrogen; Daejeon, Korea). Sequences of each were 1374 nucleotides (nt) (genome accession numbers KU140240, R007; KU140241, R041; KU140242, R-065), encoding 458 amino acids (aa; predicted size 50 kDa). Pairwise R041:R065 identities were higher (99.1 % nt, 99.6 % aa) than either R007:R041 or R007:R065 (87.3 % nt, 98.5 % aa each). Phylogenetic analysis by the Maximum-likelihood method (MEGA v.6; [26]) with 33 additional TuMV HC-Pro sequences from GenBank and *Potato virus Y* (PVY) as outgroup resulted in four TuMV clusters according to pathotype: Basal-B, World-B, Basal-BR, and Asian-BR ([17, 18]; Suppl. Table 1; Suppl. Fig. 2). The three Korean isolates grouped into the Basal-BR clade of

mainly European isolates, with 91 % bootstrap support. Apart from identities between Korean isolates, R007 was most closely related to Italian isolate ITA7 (86.5 % nt, 97.8 % aa); R041 and R065 were most closely related to Japanese isolate KWB779 J (97.7 and 97.9 % nt respectively, both 99.3 % aa)(Suppl. Fig. 2, and data not shown). Eight aa residues differentiate the Korean isolates, with six residues distinguishing R007 from both R041 and R065; R041 and R065 each differed by one residue from the consensus sequence (Suppl. Fig. 3).

HC-Pro genes of each isolate were cloned into vectors pGD (for VSR assay) and pGDG (for subcellular localization) [27] and transformed into *Agrobacterium tumefaciens* EHA105. *Agrobacterium* transformed with pGDR:Talin (actin marker), pGD:p19 [VSR of *Tomato bushy stunt virus* (TBSV)], and pGD:smGFP (soluble-modified green fluorescent protein) were also utilized [24, 28]. Equal volumes of pGDG:HC-Pro constructs and pGDR:Talin were mixed, usually with 0.1 volume of pGD:p19; agroinfiltrated leaves [28] of *N. benthamiana* were examined at 2–3 days post-agroinfiltration (dpa) using a Zeiss 710 confocal microscope [29, 30], with DAPI staining as described [31]. Imaging revealed HC-Pro of all isolates distributed throughout the cytoplasm and at the cell periphery, together with perinuclear and microfilament-like association; R007 and R041 also induced many small punctate aggregates in the cytoplasm, presumed to result from self-interaction (Fig. 1b, Suppl. Fig. 4). In contrast R065 formed punctate aggregates in few cells, and those aggregates were smaller (Fig. 1b, Suppl. Fig. 4). Western blotting showed similar HC-Pro expression levels for each isolate (Fig. 1b). Omission of pGD:p19 caused no apparent differences in HC-Pro aggregation (Suppl. Fig. 4) in contrast to [32].

Agroinfiltrations of pGD:smGFP alone, or mixed with either pGD:HC-Pro, pGD:p19, or empty pGD vector, were examined at 6 dpa under UV light; R065 HC-Pro yielded minimal enhancement of smGFP expression, whereas R007 and R041 HC-Pro significantly enhanced expression. These results were supported by qRT-PCR results (Fig. 1c), indicating that R007 and R041 HC-Pro were more effective VSRs than R007.

Because one residue (F³⁹⁵ in R007, R041; L³⁹⁵ in R065; Suppl. Fig. 3) correlated with formation of punctate HC-Pro aggregates and VSR efficiency (Fig. 1b,c), we mutated residue 395 Phe > Leu in R007 and R041 (F395L), and Leu > Phe in R065 HC-Pro (L395F) by overlap extension PCR [33] using primers shown in Table 1. Mutants were cloned into pGD and pGDG for comparison to the respective WT constructs to assay effects on HC-Pro aggregation and VSR activity. Mutants pGD:HC-Pro R007_{F395L} and R041_{F395L} had obviously reduced VSR efficiency, but R065_{L395F} gained VSR efficiency relative to

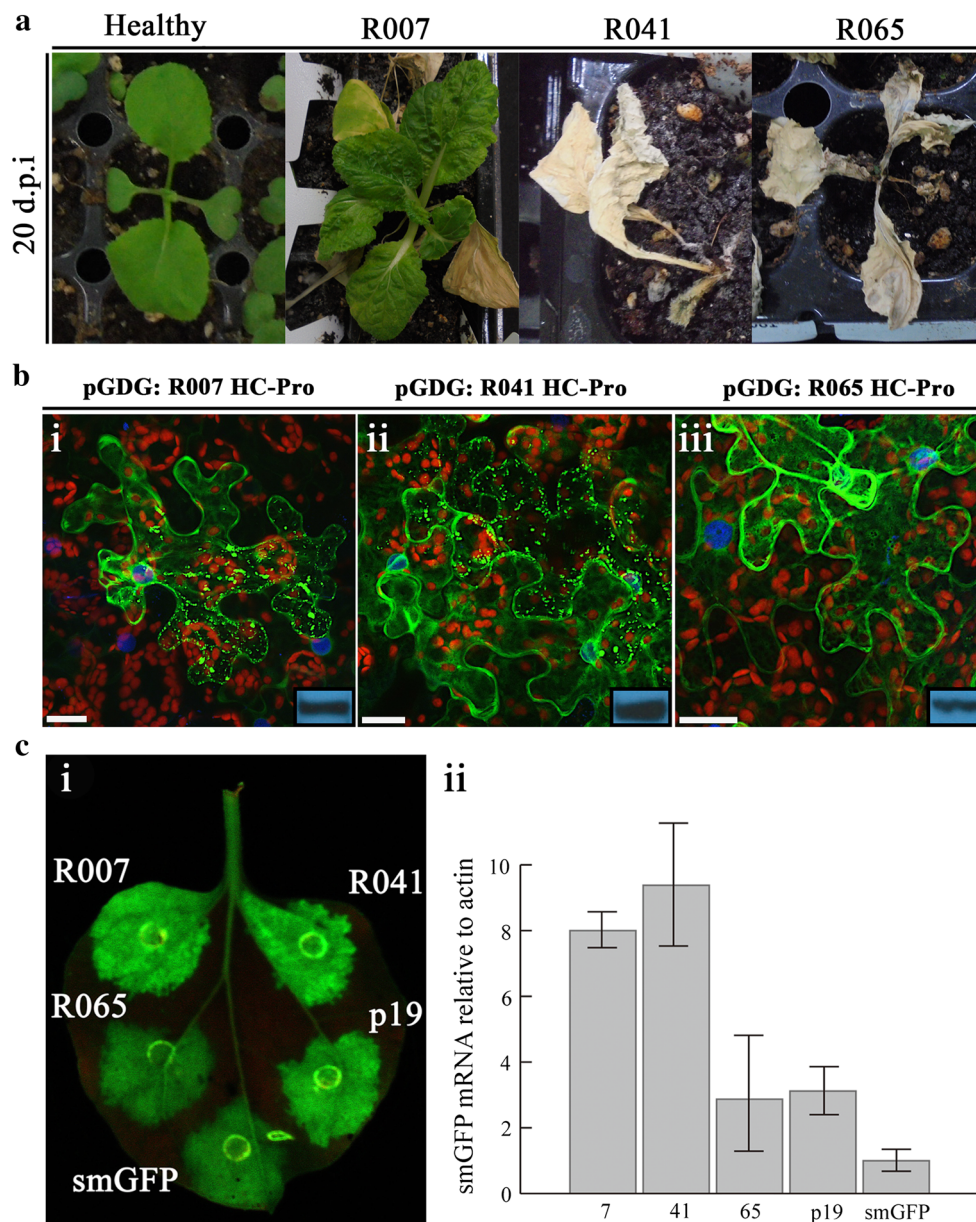


Fig. 1 a Turnip mosaic virus (TuMV) pathogenicity: Non-infected plant (Healthy) and TuMV infected (isolates R007, R041 and R065) of *Brassica rapa* ssp. *Pekinensis*: pictures taken 20 days post inoculation (d.p.i). **b** Confocal images of GFP:HC-Pro localization: pGDR:Talin and pGDG:HC-Pro of (i) R007, (ii) R041, and (iii) R065, plus pGD:p19 were agroinfiltrated to *N. benthamiana*; at 3 days after agroinfiltration, infiltrated leaves were DAPI stained. Blue color (DAPI) indicates nuclei, red color indicates chloroplast autofluorescence, green color indicates GFP:HC-Pro, and white represents DsRed:Talin. Bars indicate 20 μ m. GFP:HC-Pro protein expression was confirmed at 77 kDa by Western blot using anti GFP monoclonal

antibody (insets). **c** VSR assay (i) and quantitative RT-PCR (qRT-PCR) results (ii). i. VSR activity of TuMV HC-Pro in *N. benthamiana* leaves; pGD:TuMV HC-Pro of R007, R041 and R065, empty pGD vector, or pGD:p19 were separately co-agroinfiltrated with pGD:smGFP. R007, R041, and R065. p19 = silencing suppressor of *Tomato bushy stunt virus* used as a positive control. smGFP: smGFP co-infiltrated with empty pGD vector. ii. RNA extracts from each smGFP expressing region were subjected to qRT-PCR with smGFP specific primers. Relative RNA accumulation of smGFP was normalized to actin from two biological replicates; bars indicate standard error

the respective WT (Suppl. Fig. 5). Whereas WT pGDG:HC-Pro R007_{F395} produced many punctate aggregates (Fig. 1b, Suppl. Figs. 4,5), R007_{F395L} produced few punctate aggregates (Suppl. Fig. 5). WT R065_{L395} produced few punctate aggregates with most signal along filaments

(Fig. 1b, Suppl. Figs. 4,5), while mutant R065_{L395F} yielded obvious punctate aggregates without clear filament association (Suppl. Fig. 5). Both WT R041_{F395} and mutant R041_{F395L} produced obvious punctate aggregates scattered throughout the cytoplasm (Fig. 1b, Suppl. Figs. 4, 5).

Table 1 Primers used in this study

Target	Name	Sequence (5' → 3')	Expected size	Feature
HC-Pro	HC-Pro R7 F	AAA CTG CAG AAA TGA GCG CCG CAG GAA CCA ACT T	1374 bp	<i>PstI</i>
	HC-Pro R7 R	AAA GGA TCC CTA TCC AAC GCG GTA GTG TTT CAA G		<i>BamHI</i>
	HC-Pro F	AAA CTG CAG AAA TGA GTG CAG CAG GWG CTA ACT T		<i>PstI</i>
	HC-Pro R	AAA GGA TCC CTA WCC AAC ACG RTA GTG TTT C		<i>BamHI</i>
Poly(A)	Oligo(dT)	TTT TTT TTT TTT TTT TT	–	For cDNA synthesis
smGFP	smGFP F	TTC TCT TAT GGT GTT CAA TGC T	129 bp	For qRT-PCR
	smGFP R	GTA GTT CCC GTC GTC CTT		
Actin	Actin F	ATT GTC AGC AAC TGG GAT G	127 bp	For qRT-PCR
	Actin R	CAC GAT TAG CCT TTG GGT TA		
R007 HC-Pro	HC-Pro R7 F395L F	CTT TCT GAA AGT <u>GCT</u> TTA CCC A ^a	183 bp ^b	For construction of R007 HC-Pro F395L
	HC-Pro R7 F395L R	TGG GTA AAG <u>CAC</u> TTT CAG AAA G ^a	1194 bp ^c	
R041 HC-Pro	HC-Pro R41 F395L F	CTT TCT GAA AGT <u>GCT</u> TTA CCC T ^a	183 bp ^b	For construction of R041 HC-Pro F395L
	HC-Pro R41 F395L R	AGG GTA AAG <u>CAC</u> TTT CAG AAA G ^a	1194 bp ^c	
R065 HC-Pro	HC-Pro R65 L395F	CTT TCT GAA AGT <u>GTT</u> TTA CCC TG ^a	183 bp ^b	For construction of R065 HC-Pro L395F
	HC-Pro R65 L395R	CAG GGT AAA <u>ACA</u> CTT TCA GAA AG ^a	1194 bp ^c	

Bold type shows the recognition site of the enzyme indicated in the “Feature” column

^a Altered nucleotides for making mutant HC-Pros are underlined

^b When amplified with the respective isolate-specific HC-Pro reverse primer

^c When amplified with the respective isolate-specific HC-Pro forward primer

HC-Pro is a well-known VSR affecting viral RNA stability and replication levels, with multiple sequence differences between isolates (Suppl. Fig. 3). VSR activities of R007 and R-041 were similar, and more than twice that of R065, not corresponding with differences in SN (Fig. 1a,c). R041 and R065 HC-Pro differ by only two residues, of which only R041 Leu²⁰⁷ is in the central domain associated with VSR activity. As R065 (weak VSR) and R007 (similar to R041) have Phe²⁰⁷, this cannot explain relative VSR efficiency unless other changes in R007 compensate for ‘negative’ effects of Phe²⁰⁷. The other difference is Phe³⁹⁵ (R041) or Leu³⁹⁵ (R065) in the C-terminal protease domain. Two mutants in the central, and one in the C-terminal domain, of *Tobacco etch virus* (TEV) HC-Pro reduced both VSR activity and symptom severity; other mutants throughout TEV HC-Pro either ablated VSR activity and systemic infection or were neutral or increased both VSR and symptom expressions [34]. A mutation of the *Zucchini yellow mosaic virus* FRNK motif to FINK caused dramatic symptom amelioration in squash and ablation of symptoms in other cucurbits despite accumulation levels similar to WT [35]. Although none of the differences between R007, R041, and R065 affect any previously identified HC-Pro motifs ([8, 10–13, 15, 36–39], Suppl. Fig. 3), R065 Leu³⁹⁵ may affect HC-Pro folding, local structure, and/or self-interactions affecting VSR activity, restored in R065_{L395F} (Suppl. Fig. 5).

Subcellular aggregation of GFP:HC-Pro corresponded closely with VSR activity, suggesting a relationship between HC-Pro self-interaction and VSR activity. Lack of

R065 HC-Pro aggregation appears related to differences in self-interaction, but aggregation is not directly related to SN induction. The single C-terminal variation between R007/R041 and R065 HC-Pro (F395L) may influence self-interaction and inhibit aggregation (Suppl. Fig. 5), as this domain contributes to TuMV HC-Pro self-interaction [40]. However, R041_{F395L} reduced VSR activity but did not ablate aggregation, suggesting that L²⁰⁷ may modify the effect of F³⁹⁵ on aggregation (Suppl. Fig. 5).

Differences in GFP:HC-Pro localization correlated with differences in VSR efficiency (R007 and R041, higher VSR activity, HC-Pro aggregation; R065, weaker VSR, few punctate aggregates). However, these HC-Pro characters do not correlate with symptom severity (R041, R065 induction of SN in Chinese cabbage and *N. benthamiana*, R007 mosaic in both; this study, [25]). TuMV symptom determinants appear to be host specific, even within the *Brassicaceae*.

Different potyviral proteins affect symptoms in a host-specific manner [e.g., 41–44], and the lack of correlation between VSR efficiency and SN induction suggests that differences in viral accumulation due to HC-Pro are not responsible. We will further examine differences in HC-Pro identified here through construction of infectious clones, and substitution of different HC-Pro sequences and single residues to form chimeras in a common TuMV backbone genome. Through such studies, we hope to further advance research into TuMV biology and identify determinants of pathogenicity.

Acknowledgments This research was supported by Golden Seed Project Vegetable Seed Center (213002-04-2-WTc11), Ministry of Agriculture, Food and Rural Affairs, Korea. Mention of trade names or commercial products in this publication is solely for the purpose of providing specific information and does not imply recommendation or endorsement by the United States Department of Agriculture (USDA); USDA is an equal opportunity provider and employer.

Compliance with ethical standards

Conflict of Interest The authors declare that they have no conflict of interest.

Research involving Human Participants and/or Animals This article does not contain any studies with either human participants or animals performed by any of the authors.

References

1. K. Ohshima, M. Tanaka, N. Sako, *Arch. Virol.* **141**, 1991–1997 (1996)
2. J.A. Tomlinson, *Ann. Appl. Biol.* **110**, 661–681 (1987)
3. J.A. Walsh, C.E. Jenner, *Mol. Plant Pathol.* **3**, 289–300 (2002)
4. Z. Tan, A.J. Gibbs, Y. Tomitaka, F. Sánchez, F. Ponz, K. Ohshima, *J. Gen. Virol.* **86**, 501–510 (2005)
5. Y. Tomitaka, K. Ohshima, *Mol. Ecol.* **12**, 2099–2111 (2003)
6. F. Sánchez, X. Wang, C.E. Jenner, J.A. Walsh, F. Ponz, *Virus Res.* **94**, 33–43 (2003)
7. L. Ballut, M. Drucker, M. Pugnière, F. Cambon, S. Blanc, F. Roquet, T. Candresse, H. Schmid, P. Nicolas, O.L. Gall, S. Badaoui, *J. Gen. Virol.* **86**, 2595–2603 (2005)
8. A. Chelliah, B. Velusamy, S. Ramasamy, *Plant Pathol. J.* **14**, 123–129 (2015)
9. C. Plisson, M. Drucker, S. Blanc, S. German-Retana, O.L. Gall, D. Thomas, P. Bron, *J. Biol. Chem.* **278**, 23753–23761 (2003)
10. S. Blanc, E.D. Ammar, S. García-Lampasona, W. Dolja, C. Llave, J. Baker, T.P. Pirone, *J. Gen. Virol.* **79**, 3119–3122 (1998)
11. S. Blanc, J.J. López-Moya, R. Wang, S. García-Lampasona, D.W. Thornbury, T.P. Pirone, *Virology* **231**, 141–147 (1997)
12. Y.H. Peng, D. Kadoury, A. Gal-On, H. Huet, Y. Wang, B. Raccach, *J. Gen. Virol.* **79**, 897–904 (1998)
13. Y.M. Shibolet, E. Haronsky, D. Leibman, T. Arazi, M. Wassenegeger, S.A. Whitham, V. Gaba, A. Gal-On, *J. Virol.* **81**, 13135–13148 (2007)
14. K.D. Kasschau, S. Cronin, J.C. Carrington, *Virology* **228**, 251–262 (1997)
15. S. Cronin, J. Verchot, R. Haldeman-Cahill, M.C. Schaad, J.C. Carrington, *Plant Cell* **7**, 549–559 (1995)
16. I.G. Maia, F. Bernardi, *J. Gen. Virol.* **77**, 869–877 (1996)
17. K. Ohshima, Y. Yamaguchi, R. Hirota, T. Hamamoto, K. Tomimura, Z. Tan, T. Sano, F. Azuhata, J.A. Walsh, J. Fletcher, J. Chen, A. Gera, A. Gibbs, *J. Gen. Virol.* **83**, 1511–1521 (2002)
18. H.D. Nguyen, Y. Tomitaka, S.Y. Ho, S. Duchêne, H.J. Vetten, D. Lesemann, J.A. Walsh, A.J. Gibbs, K. Ohshima, *PLoS One* (2013). doi:10.1371/e55336
19. M.L. Shi, H.Y. Li, J. Schubert, X.P. Zhou, *Acta Virol.* **52**, 59–62 (2008)
20. H.Y. Wang, J.L. Liu, R. Gao, J. Chen, Y.H. Shao, X.D. Li, *Virus Genes* **38**, 421–428 (2009)
21. Y. Tomitaka, K. Ohshima, *Mol. Ecol.* **15**, 4437–4457 (2006)
22. K. Tomimura, J. Spak, N. Katis, C.E. Jenner, J.A. Walsh, A.J. Gibbs, K. Ohshima, *Virology* **330**, 408–423 (2004)
23. E. Kozubek, W. Irzykowski, P. Lehmann, *J. Appl. Genet.* **48**, 295–306 (2007)
24. H.S. Lim, A.M. Vaira, M.D. Reinsel, H. Bae, B.A. Bailey, L.L. Domier, J. Hammond, *J. Gen. Virol.* **91**, 277–287 (2010)
25. J.S. Chung, J.Y. Han, J.K. Kim, H.K. Ju, J.S. Gong, E.Y. Seo, J. Hammond, H.S. Lim, *Res. Plant Dis.* **21**, 235–242 (2015)
26. K. Tamura, G. Stecher, D. Peterson, A. Filipinski, S. Kumar, *Mol. Biol. Evol.* **30**, 2725–2759 (2013)
27. M.M. Goodin, R.G. Dietzgen, D. Schichnes, S. Ruzin, A.O. Jackson, *Plant. J.* **31**, 375–383 (2002)
28. H.S. Lim, J.N. Bragg, U. Ganesan, S. Ruzin, D. Schichnes, M.Y. Lee, A.M. Vaira, K.H. Ryu, J. Hammond, A.O. Jackson, *J. Virol.* **83**, 9432–9448 (2009)
29. H.S. Lim, A.M. Vaira, H. Bae, J.N. Bragg, S.E. Ruzin, G.R. Bauchan, M.M. Dienelt, R.A. Owens, J. Hammond, *J. Gen. Virol.* **91**, 2102–2115 (2010)
30. H.S. Lim, J. Nam, E.Y. Seo, M. Nam, A.M. Vaira, H. Bae, C.Y. Lee, H.G. Kim, M. Roh, J. Hammond, *Virology* **452–453**, 264–278 (2014)
31. M. Deng, J.N. Bragg, S. Ruzin, D. Schichnes, D. King, M.M. Goodin, A.O. Jackson, *J. Virol.* **81**, 5362–5374 (2007)
32. F. del Toro, F.T. Fernández, J. Tilsner, K.M. Wright, F. Tenllado, B.N. Chung, S. Praveen, T. Canto, *Mol. Plant Microbe Interact.* **27**, 1331–1343 (2014)
33. R. Higuchi, B. Krummel, R.K. Saiki, *Nucleic Acids Res.* **16**, 7351–7367 (1988)
34. C. Torres-Barceló, Martín S, J. A. Daròs, S. F. Elena. *Genetics* **180**, 1039–1049 (2008)
35. A. Gal-On, *Phytopathology* **90**, 467–473 (2000)
36. C.S. Oh, J.C. Carrington, *Virology* **172**, 692–699 (1989)
37. M. Ala-Poikela, E. Goytia, T. Haikonen, M. Rajamäki, J.P.T. Valkonen, *J. Virol.* **85**, 6784–6794 (2011)
38. S.K. Mangrauthia, R.K. Jain, S. Praveen, *J. Plant Biochem. Biotechnol* **17**, 201–204 (2008)
39. H. Huet, A. Gal-On, E. Meir, H. Lecoq, B. Raccach, *J. Gen. Virol.* **75**, 1407–1414 (1994)
40. H. Zheng, F. Yan, Y. Lu, L. Sun, L. Lin, L. Cai, M. Hou, J. Chen, *Virus Genes* **42**, 110–116 (2011)
41. P. Sáenz, M.T. Cervera, S. Dallot, L. Quiot, J.B. Quiot, J.L. Riechmann, J.A. García, *J. Gen. Virol.* **81**, 557–566 (2000)
42. S. Dallot, L. Quiot-Douine, P. Sáenz, M.T. Cervera, J.A. García, J.B. Quiot, *Phytopathology* **91**, 159–164 (2001)
43. B. Salvador, M.O. Delgadillo, P. Sáenz, J.A. García, C. Simón-Mateo, *J. Gen. Virol.* **81**, 557–566 (2008)
44. A. Nagyová, M. Kamencayová, M. Glasa, Z.W. Subr, *Virus Genes* **44**, 505–512 (2012)